X-621-76-290
PREPRINT

NASA TM X- 71251

WIND ENHANCED PLANETARY ESCAPE: COLLISIONAL MODIFICATIONS

S. A. CURTIS
R. E. HARTLE

DECEMBER 1976

GSFC — GODDARD SPACE FLIGHT CENTER —
GREENBELT, MARYLAND

X-621-76-290
Preprint

WIND ENHANCED PLANETARY ESCAPE: COLLISIONAL MODIFICATIONS

S. A. Curtis
R. E. Hartle

December 1976

GODDARD SPACE FLIGHT CENTER
Greenbelt, Maryland

WIND ENHANCED PLANETARY ESCAPE:
COLLISIONAL MODIFICATIONS

ABSTRACT

The problem of thermal escape is considered in which both the effects of thermospheric winds at the exobase and collisions below the exobase are included in a Monte Carlo calculation. The collisions are included by means of a collisional relaxation layer of a background gas which models the transition region between the exosphere and the thermosphere. The wind effects are considered in the limiting cases of vertical and horizontal flows. Two specific species are considered: terrestrial hydrogen and terrestrial helium. In the case of terrestrial hydrogen the escape fluxes were found to be strongly filtered or throttled by collisions at high exospheric temperatures. The ratio of escaping flux to total upward flux at the exobase is found to approach a limiting value significantly less than unity. Collisional filtering of particles exceeding the escape velocity greatly reduces the enhanced H escape that would otherwise be produced by winds. Such a drastic reduction in escape by collisions occurs even for winds near the sound speed. For terrestrial helium, departures from previous predictions for collisionless wind enhanced escape are found to be insignificant at exospheric temperatures less than 5000°K. Thus, even with collisions, wind enhanced escape could be a significant helium loss mechanism contributing to the helium budget. In the case of terrestrial hydrogen, the mass of the background gas comprising the relaxation layer is varied from 1 to 44 amu. The result is increased throttling with increasing background

mass, the effect being larger at lower temperatures. Finally, the model is applied to molecular hydrogen diffusing through a methane relaxation layer under conditions possible on Titan. The results are similar to the case of terrestrial hydrogen with wind enhanced escape being strongly suppressed by collisions. It is concluded that wind enhanced escape is not an important process on Titan.

CONTENTS

LIST OF ILLUSTRATIONS

Introduction

An understanding of the processes by which a constituent of a planetary atmosphere can escape is fundamental for the interpretation of the observed abundances in the terrestrial atmosphere as well as in placing limits on the expected abundances of the atmospheric constituents of other planets and their satellites. It is in this sense that escape processes form a basic building block in the construction of theories of atmospheric evolution.

Historically, one of the earliest and most frequently used models for thermal escape was that derived by Jeans (1916). Jeans considered the simplest physical model in which a Maxwellian flux of particles in the upward direction resides at the exobase, the base of the collisionless part of the atmosphere, the exosphere. No bulk flow of the atmosphere below the exobase was considered. The ratio of the escaping flux, Φ_J, to the upward flux, Φ_{up}, was found to be:

$$\frac{\Phi_J}{\Phi_{up}} = (1 + \alpha)e^{-\alpha}$$

where $\alpha = GMm/RkT$, G is the gravitational constant, M is the planetary mass, m is the constituent mass, R is the planetary radius, k, the Boltzmann constant and T, the exobase temperature. Thus, α is proportional to an atom's ratio of its gravitational energy to its kinetic energy and is the characteristic parameter in the escape process.

More recently, the effects of the gradual relaxation of the gas from a collision dominated state to a collisionless one have been considered by Chamberlain and Campbell (1967) and Brinkmann (1970). The

effect of the inclusion of such a relaxation layer is to reduce the escaping flux below the Jeans value for a light gas such as terrestrial hydrogen. For heavier gases such as terrestrial helium the effect of collisions is almost negligible. What determines the lightness or heaviness of an atmospheric constituent is both the magnitude of the gravitational potential the atom or molecule resides in as well as the range of temperatures in the ambient atmosphere. For example, a hydrogen atom would be relatively heavy in the Jovian exosphere while an argon atom would be light on the largest asteroid, Ceres. The previously defined parameter α effectively determines the lightness (small α) or heaviness (large α) of an atomic or molecular species in a given planetary atmosphere. These prior results that include collisions can then be interpreted as meaning that collisional effects are significant for species with small α, values less then those which characterize terrestrial helium.

In addition to collisions, the effect of non-zero bulk flow, or winds, on thermal escape have been considered by Hartle and Mayr (1976). Here the specific case of terrestrial helium was considered. The escape processes of helium are of particular importance and interest due to their bearing on the question of the terrestrial helium budget. From these calculations Hartle and Mayr found that, for relatively high winds, large enhancements over the Jeans escape flux are possible. The enhancement increases as the wind velocity increases and as the constituent's α increases.

It is our purpose here to consider both the effects of collisions and finite winds simultaneously. We will specifically consider the cases of terrestrial hydrogen and helium. The method of calculation we

employ is similar to that of Brinkmann in that a Monte Carlo approach is adopted. We will consider winds characteristic of a highly perturbed atmosphere and examine the extent to which the earlier calculations of collisionless wind enhancement require corrections due to collisional effects. Two limiting cases are considered: those of vertical and horizontal winds.

Method of Calculation

We model the relaxation layer between the collisionless exosphere and the collision dominated thermosphere as a slab of column density 10^{15} cm^{-2}, with a depth of 10^{7} cm and a uniform density of 10^{8} cm^{-3}. The slab geometry is shown in Figure 1. Terrestrial hydrogen and helium are regarded as minor constituents diffusing through a background gas of atomic oxygen at a fixed temperature. A position in this layer is thus a measure of optical rather than physical depth. The justification of the layer thickness is shown a posteriori: at the end of the calculation the downward flux distribution at the bottom of the slab is found to be Maxwellian like the injected flux to within the accuracy of our results.

The plane parallel geometry of the slab is used as the thickness of the relaxation layer is small compared to the planetary radius for the cases considered.

The minor constituent's speed is chosen from a Maxwellian flux distribution and is injected through the relaxation layer's base. After the injection, the atom is followed until it either escapes through the top of the relaxation layer with energy greater than the escape energy and hence is lost from the atmosphere or until it reenters the thermosphere below the relaxation layer. It is in the escape energy calculation

that the effect of the non-zero wind velocity, $\underset{\sim}{U}$, enters. In the vanishing wind case all directions require equal escape energy at the relaxation layer's top in the hemisphere about the slab normal pointing into the exosphere. For finite winds this isotropy is broken and the escape energy is minimal along the wind direction. This anisotropy requires a fully three dimensional layer in which not only the zenith angle θ and distance in the slab z are recorded, but also the azimuthal angle ϕ. As the minor constituent randomly walks through the relaxation layer it suffers a number of collisions with the background gas. To compute the atom's new velocity, $\underset{\sim}{V}'_H$, it is desireable to transform from the slab frame moving with velocity $\underset{\sim}{U}$ to a frame moving with the wind speed whose Z axis lies along the relative velocity vector, $\underset{\sim}{V}_r = \underset{\sim}{V}_H - \underset{\sim}{V}_o$, where $\underset{\sim}{V}_H$ and $\underset{\sim}{V}_o$ are the initial velocities of the minor and background gas constituents respectively. This is the laboratory frame system. The scattering angle is chosen as a random deviate between 0 and $\pi/2$ in the center of mass frame and then transformed to the laboratory system. The angular dependences of the collision cross sections are neglected as a result of the earlier results of Brinkmann, that showed them to be insignificant. The minor constituent atom velocity is calculated directly from the momentum and energy conservation relations for the collisions. The resulting new velocity of the minor constituent is then transformed back to the slab frame and the new polar angles θ' and ϕ' are computed. If the atom does not meet the criteria for leaving the slab either by escape or reentry, it continues its random walk in the relaxation layer. If the atom is lost a new randomly chosen atom is injected at the relaxation layer's base.

The detailed methods of randomly selecting the injected atom's velocity and the minor-background gas collision dynamics with their associated mean free path calculations that we employ here follow closely those of Brinkmann. For this reason we refer the reader to that paper and do not reproduce the details here. We note, however, that the calculation mechanics do differ significantly from Brinkmann's in that the process we use here is fully three dimensional as necessitated by the angular anisotropy of the escape energies. In addition, we note that when generating the tables for the randomly chosen velocities and mean free paths that we use in these calculations, we pay particular attention to the tables' accuracy in the high energy tail of the atom's velocity distribution function. In our calculations, the tables employed have both a much smaller spacing between tail interpolation points and many more points in the tail at higher energies than the tables employed by Brinkmann. This enables us to obtain much greater inherent precision in these Monte Carlo calculations using injection from the lower boundary of the relaxation layer as is required in non-zero wind cases. The reasons for this stems from two limitations on the precision of these Monte Carlo calculations. The first and most obvious limitation is that due to the signal to noise ratio resulting from the number of counts, N, for a given event. In our case the events are escapes. This obstacle to precision is removable however given sufficient computer time. The relative error decreases like $N^{-1/2}$. The second limitation is due to a quantization effect, the coarseness with which the model parameters are randomly chosen. Thus for a coarse interpolation grid a relatively low level of precision is obtainable in the long computation time limit.

The interpolation tables cannot, however, be made arbitrarily large due to finite computer storage. Thus, in a spirit of economy, we have chosen table sizes which provide an inherent precision of about one percent and perform calculations yielding about a five percent precision.

The mechanics of the Monte Carlo computer experiment are as follows: We inject minor constituent atoms one at a time in groups of 10^3 and record the number escaping η_{esc}, the escaping flux

$$\Phi_{esc} = \sum_i V_i \qquad i = 1 \text{ to } \eta_{esc},$$

the upward injected flux at the base

$$\Phi_{up} = \sum_i V_i \qquad i = 1 \text{ to } 10^3$$

and other results of interest such as the upward and downward flux distributions at various relaxation layer depths. The ratio of escaping flux to injected flux, Φ_{esc}/Φ_{up} was also computed. In general about 10^4 trajectories were followed for each case of interest. From the groups of 10^3, $< \Phi_{esc}/\Phi_{up} >$ was computed which is taken as the escape factor. The standard deviation is also calculated for an estimate of precision. The final flux distributions are simply the sum of the flux distributions for all the injected groups of a given case.

Results

Monte Carlo computer experiments were performed for terrestrial hydrogen with exobase temperatures T greater than 1000°K and for terrestrial helium with $T \geq 5000$°K. We have chosen these temperatures ranges as they represent the temperature regimesin which significant departures from collisionless wind enhanced escape arise from the inclusion of

collisions. The normalized wind speeds u we use in these calculations range from 0 to 1.0. Here, u is the wind speed U expressed in units of the minor constituent thermal velocity, $\underset{\sim}{V}_{th}$:

$$u = U/V_{th}$$

$$V_{th} = (2kT/m)^{1/2}$$

where m is the minor species mass.

In Figure 2, we show for comparison, flux distributions in the relaxation layer for the case of terrestrial atomic hydrogen with a horizontal wind, u = 1.0. The large horizontal wind magnitude is chosen for demonstration purposes. Specifically, the upwardly injected flux distribution at the relaxation layer's bottom, which is drawn randomly from a parent Maxwellian flux distribution, is compared with the returning downward flux distribution at the base of the relaxation layer. The two flux distributions agree to within the limits of precision of the results of the computer experiment. We have compared the upward and downward flux distributions for the range of temperatures we use here and have found close agreement between them, allowing us to conclude that the relaxation layer is of sufficient depth to attain a Maxwellian distribution at the layer's base.

Again, for the case of terrestrial hydrogen, we show in Figure 3 the downward flux distribution F_{DT}, at the relaxation layer's top and compare it with the upwardly injected Maxwellian flux distribution at the layer's base, F_{INJ}. Two effects are immediately obvious from this comparison. The first is the large decrease of the F_{DT} as compared to F_{INJ} at speeds in the vicinity of and greater than the terrestrial

escape speed V_{esc} due to wind enhanced escapes. The second is that rather than there being a sharp step function cutoff in F_{DT} at the escape velocity, as is seen in the windless cases of Chamberlain and Campbell (1967) there is a more gradual decrease of the flux distribution to zero over the speed range V_{esc} -U to V_{esc} +U for the horizontal wind used in this example. This effect is understandable since the escape velocity for non-zero wind speeds is not isotropic and in the specific case of horizontal winds ranges from V_{esc} -U to V_{esc} +U. Thus, on all rotating planets, as there exists an effective horizontal wind when the atmosphere is viewed from an inertial frame, the F_{DT} cutoff will not be abrupt but go to zero over an interval $2U_{rot}$ centered at the inertial frame escape velocity. Here U_{rot} is the exospheric rotational velocity at the latitude of interest.

Turning from these microscopic results to macroscopic ones, in Figure 4 we display the simulation results for terrestrial hydrogen for various horizontal wind speeds. Here we have the escape factor $\langle \Phi_{esc}/\Phi_{up} \rangle$ for wind speeds between u = 0 and u = 1.0. The collisional results are compared with earlier collisionless results with u = 0 in the collisionless case representing Jeans escape and u $\neq$ 0 corresponding to the results of Hartle and Mayr. As the exobase temperature, T, increases we observe an increasing departure of the collisionless results from the collisional results that we compute here. What one observes is the throttling of the escape process by collisions, resulting in a limiting escape factor at high exobase temperatures of only about .3 of what is predicted by the collisionless models for even the very high wind case of u = 1.0.

In Figure 5 we again display results for terrestrial hydrogen but in this case for vertical winds. We also find the escape factor approaches the same limiting value of .3, significantly less than the value of unity predicted by the collisionless theories. We conclude that throttling is also effective for vertical winds. (Note that the escape factors of Hartle and Mayr have been multiplied by the factor $(\exp(-u^2) + \pi^{1/2} u[1 - \mathrm{erf}(u)])^{-1}$ to account for the proper contribution of the bulk motion caused by the vertical winds.) Before the limiting factor is approached we observe that vertical winds are more efficient in increasing the escape factor than a horizontal wind of equal speed. This is explicable from a microscopic viewpoint since antiparallel alignments with horizontal winds are possible but are not with vertical winds in the upward flux that contributes to the escape flux.

We now consider the case of terrestrial helium. As shown in Figure 6 significant departures from the predicted escape factors of collisionless models (Hartle and Mayr $u \neq 0$; Jeans, $u=0$) do not occur until very high exobase temperatures are attained, $T \gtrsim 6000°K$. This is true for both horizontal and vertical winds, even in the high wind case of $u = 1.0$. We conclude that $\langle \Phi_{esc}/\Phi_{up} \rangle$ is accurately given by the collisionless model for terrestrial helium when $T \lesssim 5000°K$. The possibility of very large increases of the escape factor by high winds (Hartle and Mayr, 1976), perhaps realizable under very perturbed atmospheric conditions, remains admissable. Large wind enhancements of terrestrial helium escape factors therefore remain potentially important in considerations of the helium budget (e.g.; Hartle and Mayr, 1976; MacDonald 1963).

In Figure 7 we display the collisional wind enhanced escape factors for both terrestrial helium and hydrogen for vertical and horizontal winds and compare these with the classical Jeans escape factors. Here we have $<\phi_{esc}/\phi_{up}>$ as a function of α. We note that when viewed as a function of α the behavior of each of the two species is quite similar. Both helium and hydrogen exhibit the same limiting behavior induced by collisional throttling at sufficiently low α and the factors are less than those of the classical Jeans theory even for $u = 1.0$. The difference between these two gases is that for terrestrial helium the low α regime is most likely not realizable.

In viewing the limiting behavior of terrestrial helium and hydrogen at low α we note from Figure 7, that the limiting factors approached are different. This occurs due to the different mass ratios of the diffusing gases to the background gas. In Figure 8 we have examined the effect of varying the mass of this background gas for the case of atomic hydrogen as the minor constituent. The background masses are varied from zero amu, corresponding to the collisionless case, to 44 amu, the mass of carbon dioxide. The case of atomic hydrogen diffusing through CO_2 has been previously considered by Chamberlain (1969). We note that the escape factor decreases more rapidly for a given increase in the background mass at lower wind speeds and lower temperatures than it does at higher speeds and higher temperatures. We note also that significant collisional attenuation of $<\phi_{esc}/\phi_{up}>$ can occur even when the background gas has the same mass as the minor diffusing constituent.

As an example of the extension of this technique to other planets, we consider the case of Titan, Saturn's satellite with a substantial atmosphere. Specifically, we consider the relaxation layer at one planetary radius from the surface, a temperature of 165°K, a background gas of CH_4 (mass = 16 amu) and a minor constituent of H_2 (mass = 2 amu). This yields $\alpha = 1.14$ and a Jeans escape factor of .68. By direct computation we find the escape factor is .33 for both horizontal and vertical winds with u = 1.0. We conclude that wind enhanced escape is negligible on Titan for this parameter, the escaping H_2 being strongly throttled by the background CH_4. This result could also be inferred directly by inspection of Figure 7, noting that the background mass dependence of the throttling effect is relatively weak. Using $\alpha = 1.14$ and observing that the mass ratio $H_2/CH_4 = 1/8$ is midway between He/O = 1/4 and H/O = 1/16 a crude guess would be .3 in close agreement with the direct result.

Conclusion

We have demonstrated that the inclusion of collisions in the escape model for terrestrial hydrogen with winds effectively throttles the escape process. The limiting escape factor in the high exobase temperature limit is found to be significantly less than that predicted by collisionless models. In contrast, in the case of terrestrial helium, we find that for the accepted range of exobase temperatures the collisional throttling or filtering of wind enhanced escape is negligible. This implies that the earlier predictions of Hartle and Mayr (1976) of potentially large wind enhancements in helium escape as well as their application to the terrestrial helium budget remain valid.

Finally, we have found the escape of a constituent of a planetary atmosphere to depend both on its ratio of gravitational energy to kinetic energy as well as the ratio of its mass to that of the background gas. The strongest dependence we find is on α.

REFERENCES

Brinkmann, R. T., Departures from Jeans' escape rate for H and He in the Earth's atmosphere, Planet. Space Sci., 18, 449-478, 1970.

Chamberlain, J. W. and Campbell, F. J., Rate of evaporation of a non-Maxwellian atmosphere, Astrophys. J., 149, 687, 1967.

Chamberlain, J. W., Escape rate of hydrogen from a carbon dioxide atmosphere, Astrophys. J., 155, 711, 1969.

Hartle, R. E. and Mayr, H. G., Wind-Enhanced escape with application to terrestrial helium, J. Geophys. Res., 81, 1207, 1976.

Jeans, J. H., Dynamical Theory of Gases, Cambridge University, Press, London, 1916.

MacDonald, G. J. F., The escape of helium from the Earth's atmosphere, Rev. Geophys., 1, 305, 1963.

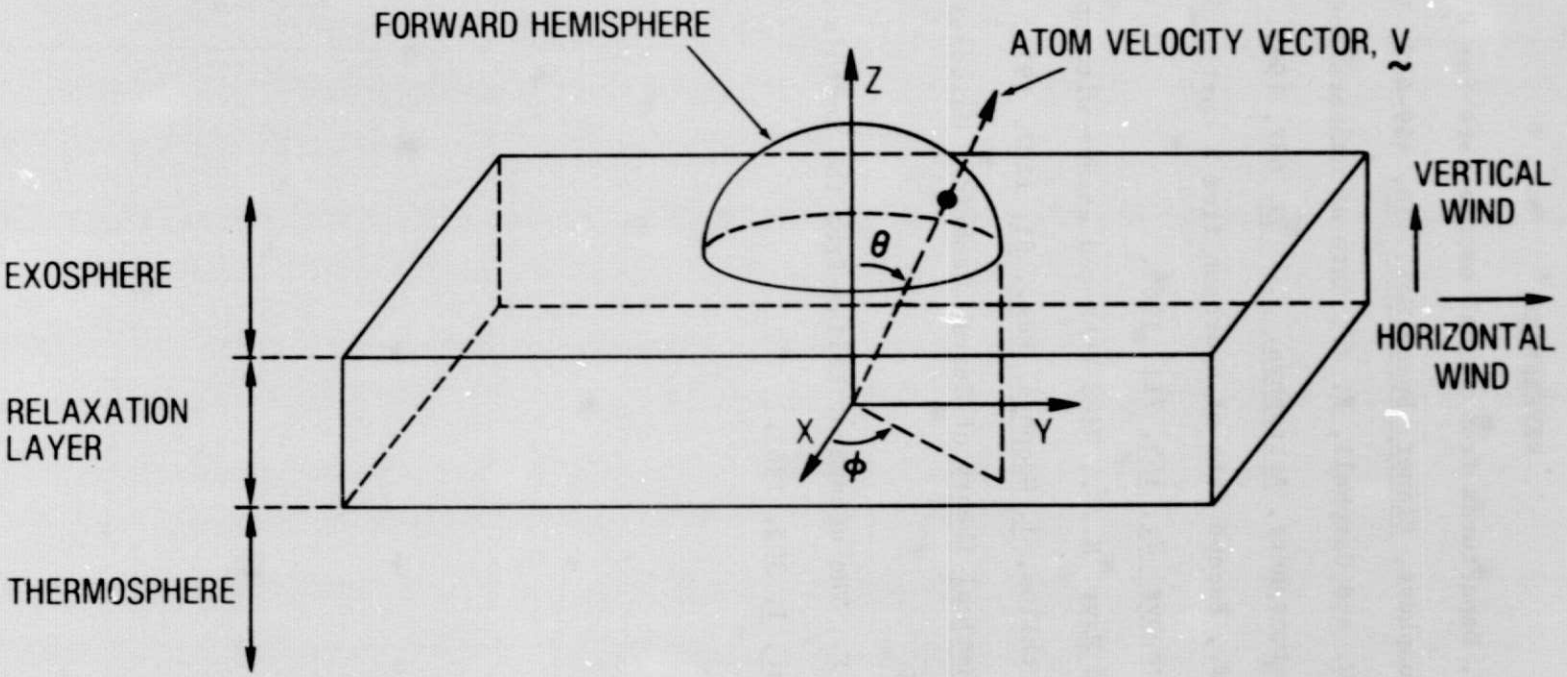

Figure 1. Slab geometry used in Monte Carlo calculations.

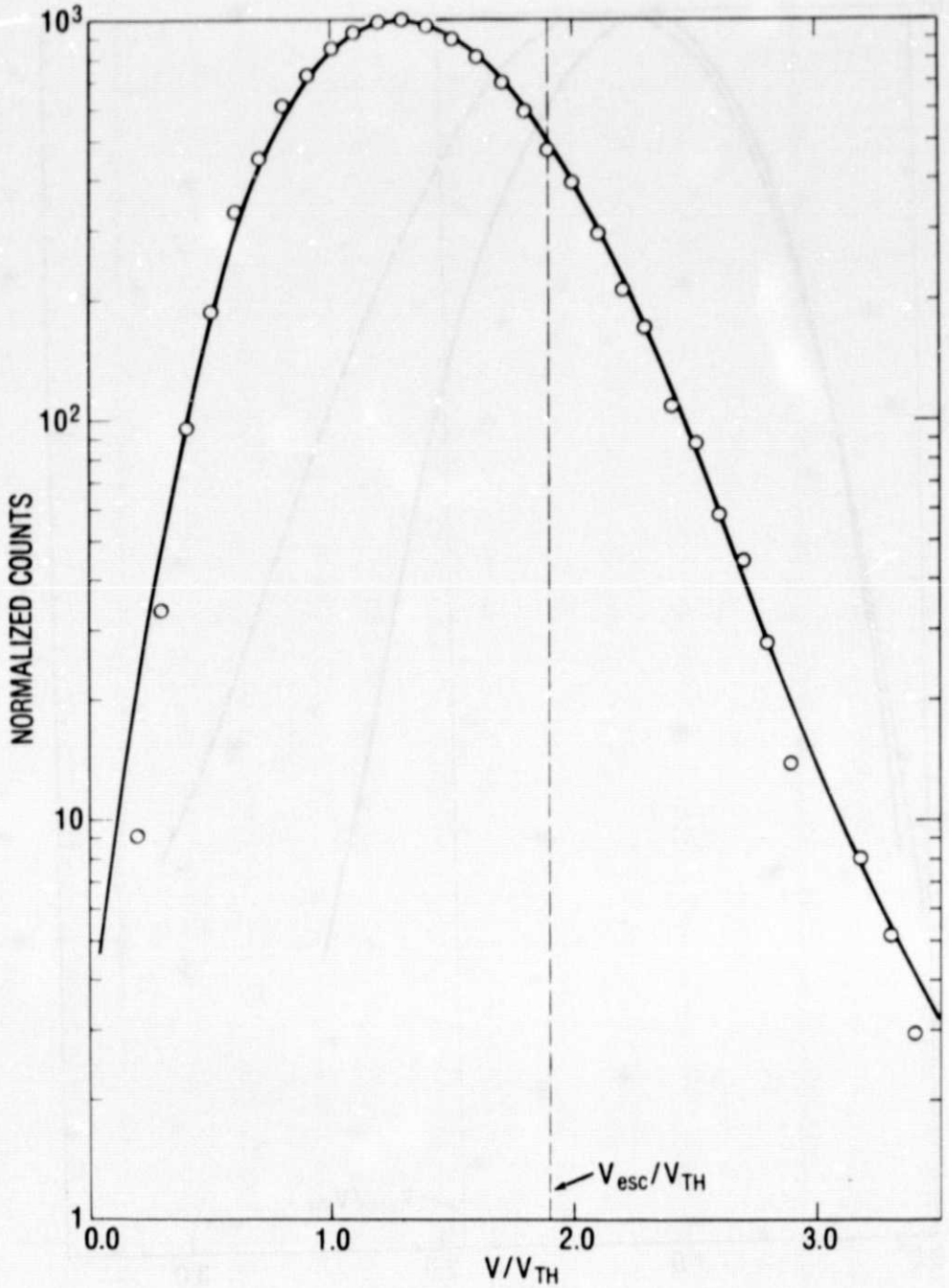

Figure 2. Flux distributions for terrestrial atomic hydrogen in an atomic oxygen relaxation layer for T = 2000°K and a horizontal wind speed u = 1.0. The solid line represents the upward flux distribution at the layer's bottom and the open circles, the downward flux at the layer's bottom. The velocity scale is normalized by $V_{th} = (2kT/m_H)^{1/2}$.

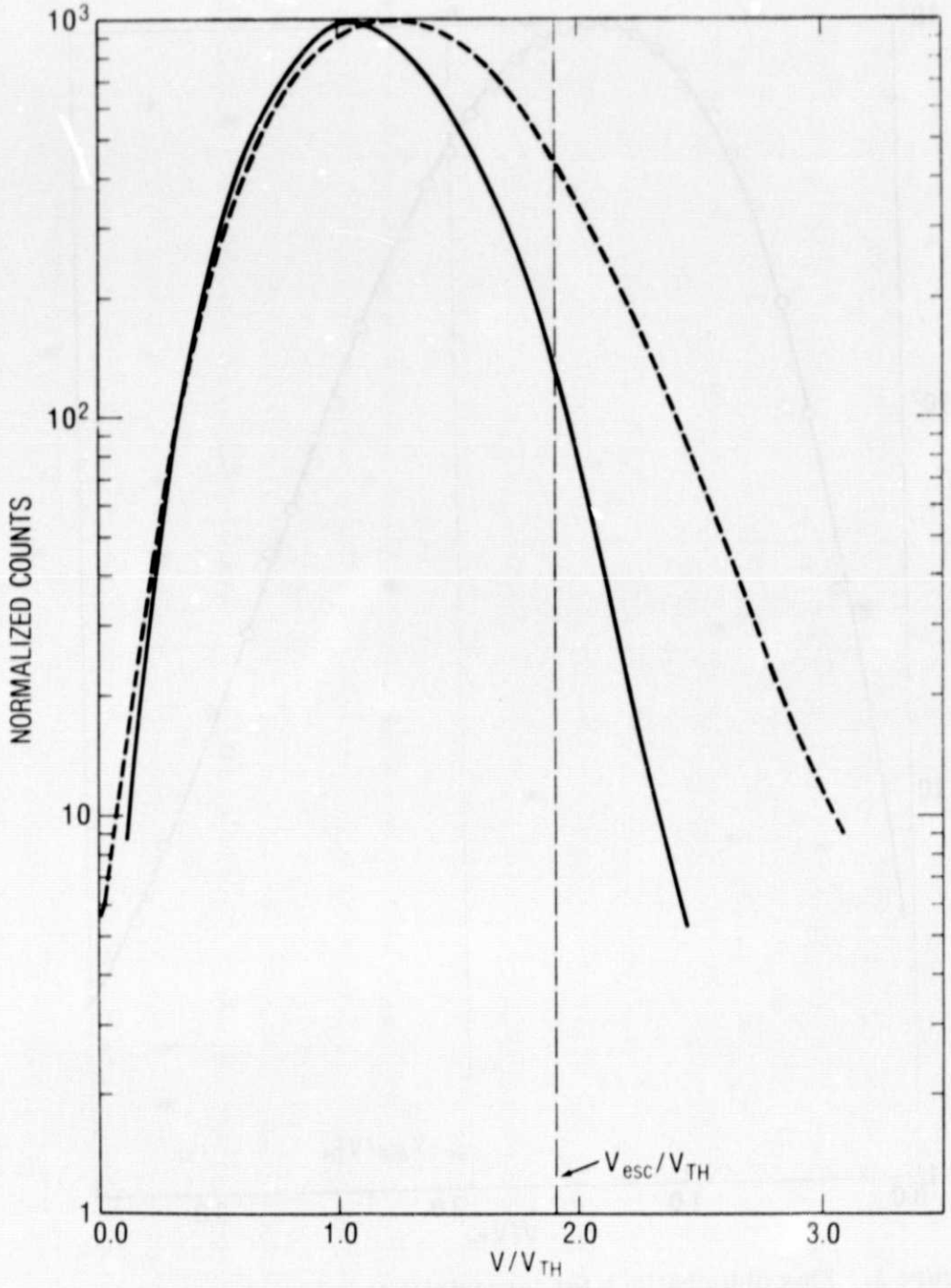

Figure 3. Comparison of the downward flux distribution at the layer top (solid line) and the upward flux distribution at the relaxation layer bottom (dotted line) for terrestrial hydrogen. Here T = 2000° K and the horizontal wind speed is u = 1.0. The velocity scale is normalized by $V_{th} = (2kT/m_H)^{1/2}$.

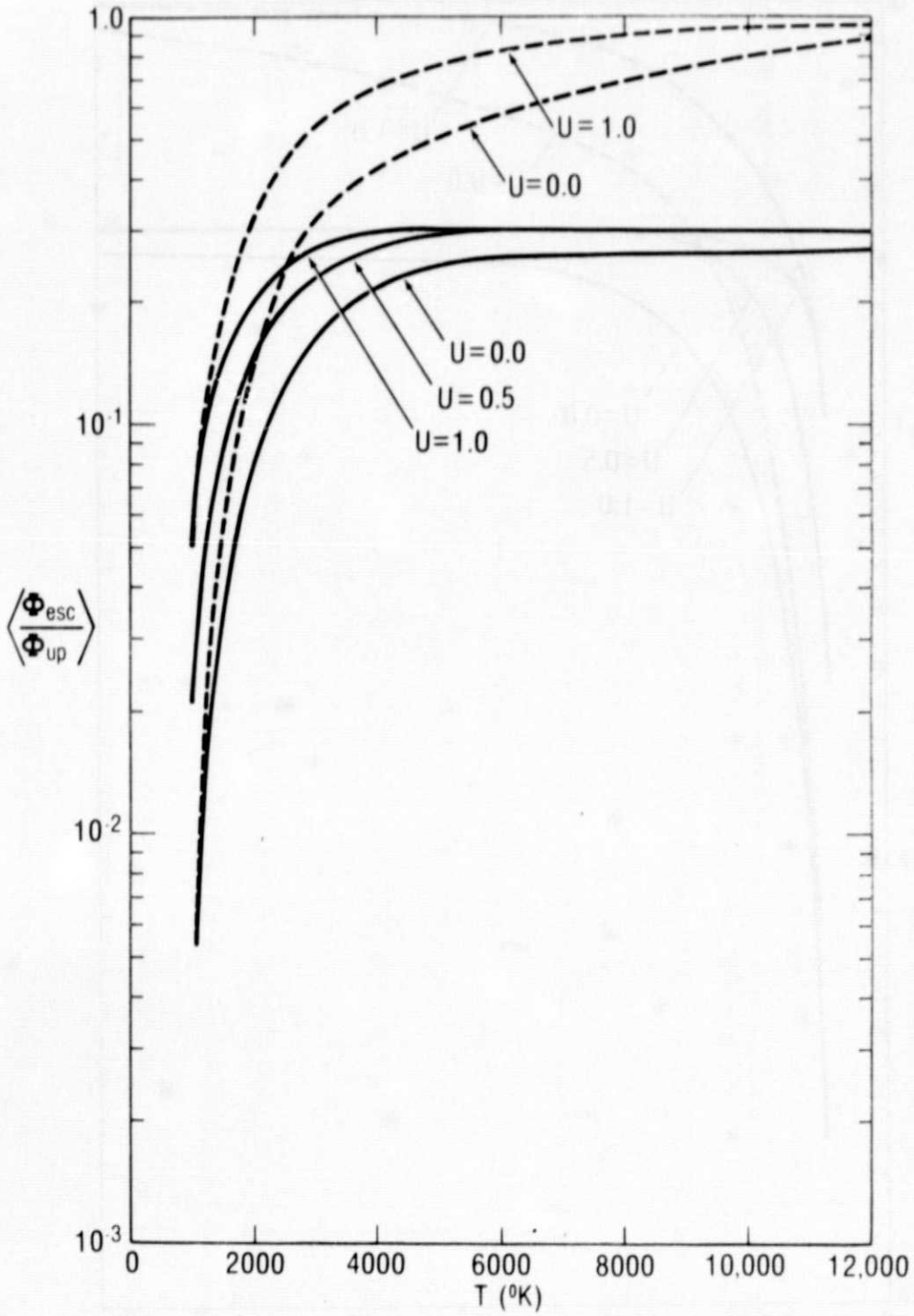

Figure 4. Terrestrial hydrogen with horizontal winds, u, in an atomic oxygen relaxation layer. The collisionless (dotted lines) and collisional (solid lines) escape factors are displayed.

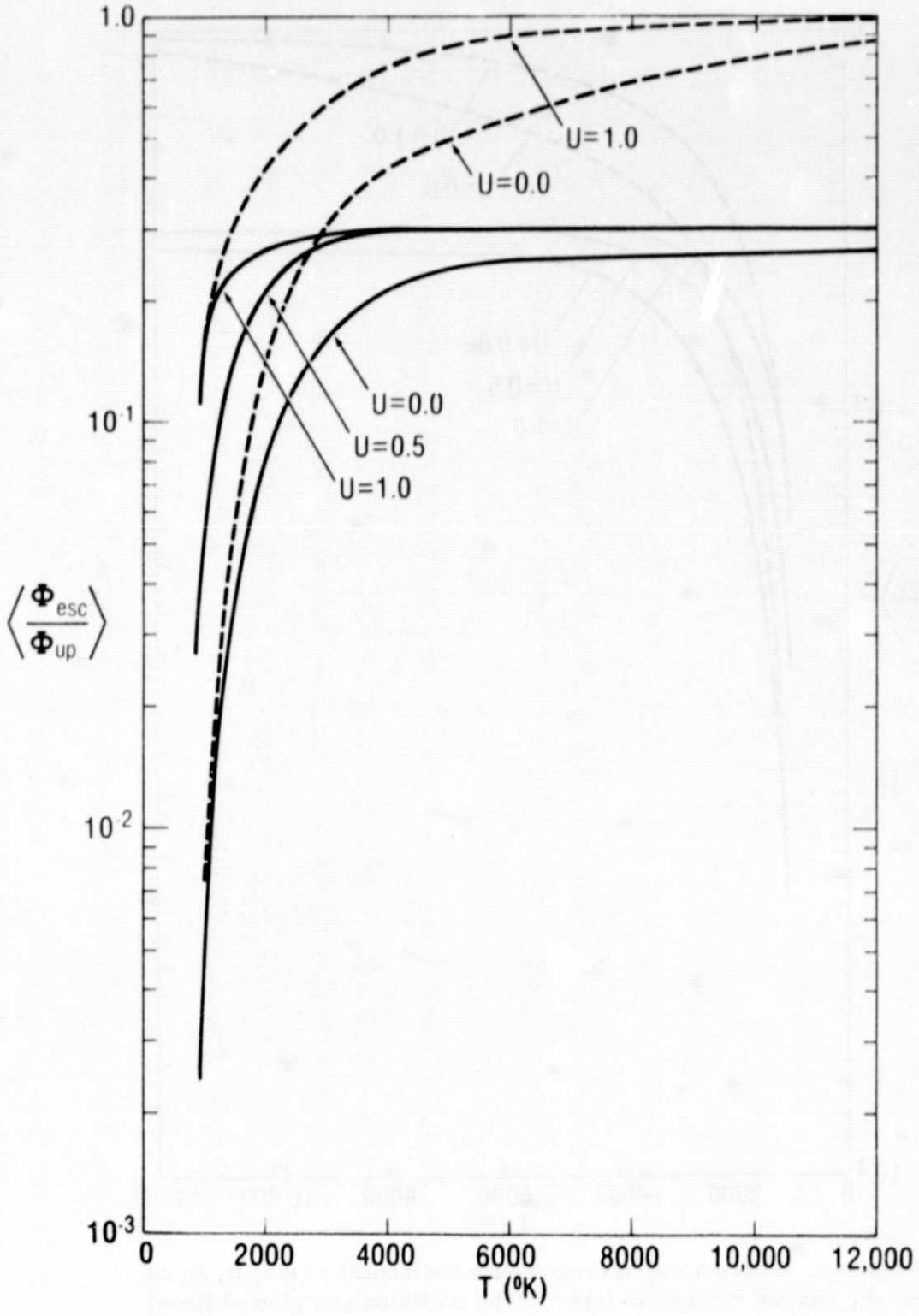

Figure 5. Same as Figure 4 but for vertical winds.

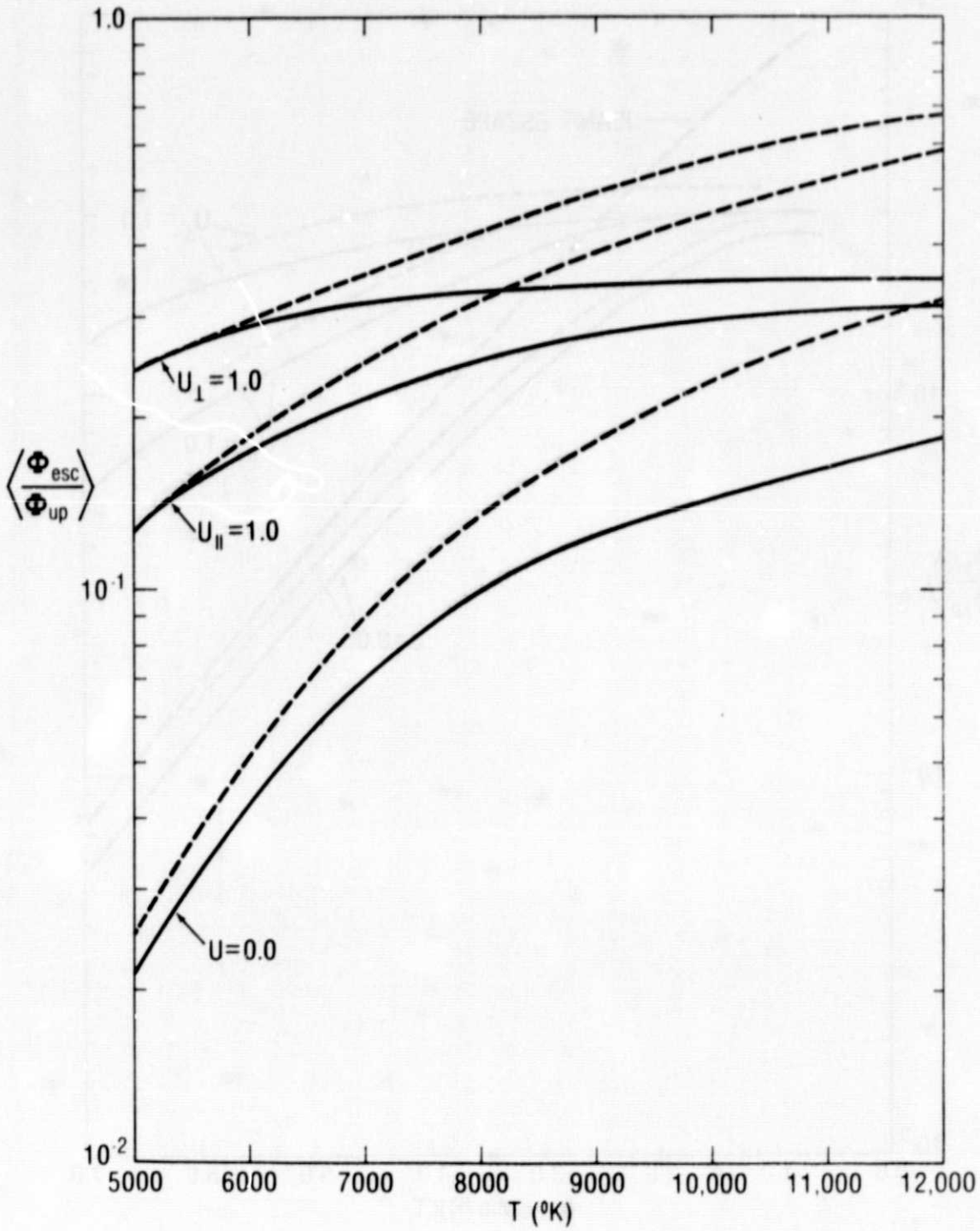

Figure 6. Terrestriai helium in an atomic oxygen relaxation layer. The results for both collisionless (dotted lines) and collisional (solid lines) cases are displayed for selected values of $u_\perp$ (vertical wind) and $u_\parallel$ (horizontal wind).

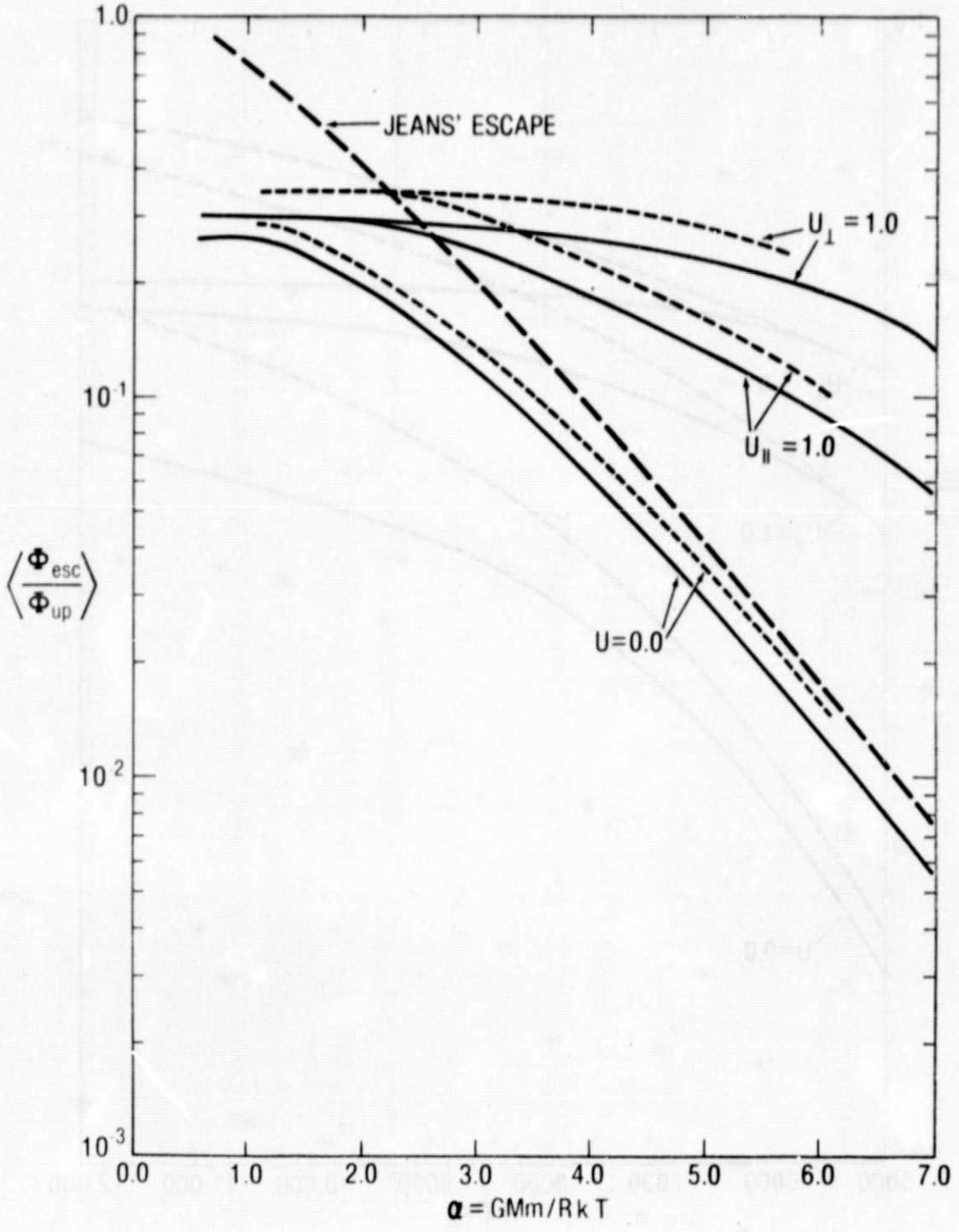

Figure 7. Comparison of terrestrial hydrogen (solid lines) and helium (dotted lines) in an atomic oxygen relaxation layer as functions of the parameter, α. The Jeans result is shown also.

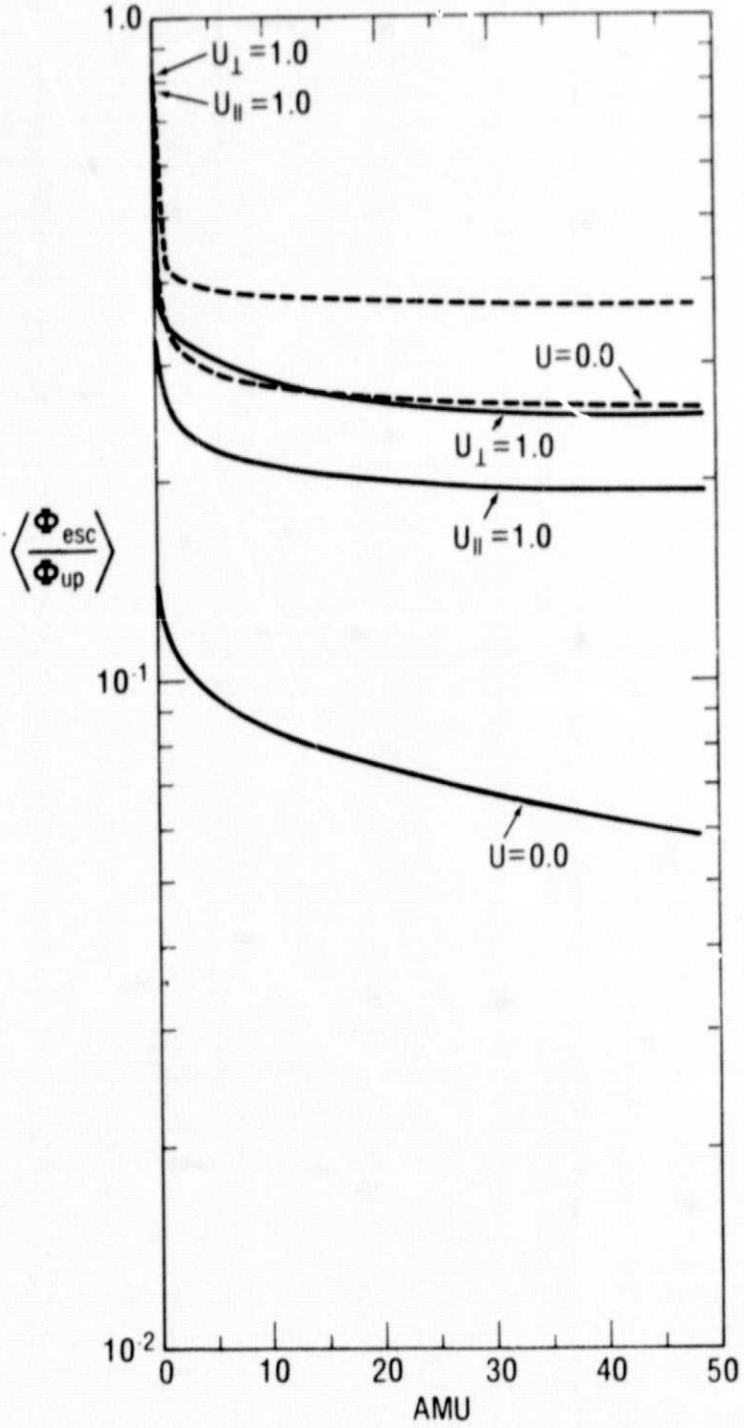

Figure 8. The effect of varying the mass of the relaxation layer constituent on the escape of terrestrial hydrogen is shown for T = 2000°K (solid line) and T = 5000°K (dotted line).